Corrosion characteristics of reduced activation ferritic steel, JLF-1 (8.92Cr–2W) in molten salts Flibe and Flinak

Masatoshi Kondo[a,b,*], Takuya Nagasaka[a,b], Qi Xu[b], Takeo Muroga[a,b], Akio Sagara[a,b], Nobuaki Noda[a], Daisuke Ninomiya[c], Masaru Nagura[c], Akihiro Suzuki[c], Takayuki Terai[c], Naoki Fujii[d]

[a] National Institute for Fusion Science, Oroshi, Gifu, Japan
[b] The Graduate University for Advanced Studies, Toki, Gifu, Japan
[c] University of Tokyo, Tokyo, Japan
[d] Biko Chemical Company, Koube, Japan

ARTICLE INFO

ABSTRACT

Static corrosion tests were performed in molten salts, LiF–BeF$_2$ (Flibe) and LiF–NaF–KF (Flinak), at 500 °C and 600 °C for 1000 h. The purpose is to investigate the corrosion characteristics of reduced activation ferritic steels, JLF-1 (8.92Cr–2W) in the fluids. The concentration of hydrogen fluoride (HF) in the fluids was measured by slurry pH titration method before and after the exposure. The HF concentration determined the fluoridation potential. The corrosion was mainly caused by dissolution of Fe and Cr into the fluids due to fluoridation and/or electrochemical corrosion. Carbon on the surface might be dissolved into the fluids due to the corrosion, and this resulted to the decrease of carbide on the surface. The corrosion depth of the JLF-1 specimen, which was obtained from the weight losses, was 0.637 μm in Flibe at 600 °C and 6.73 μm in Flinak at 600 °C.

1. Introduction

Force free helical type reactor (FFHR) with liquid blanket system has been designed. Molten salt Flibe (LiF–BeF$_2$) is planed to be used as tritium (T) breeder and coolant of the blanket [1]. Corrosion of the structural materials in Flibe is one of critical issues.

Corrosion of the structural material in Flibe is caused by fluoridation due to the chemical reaction with tritium fluoride (TF), which is generated in Flibe according to the neutron irradiation during the operation. The corrosion is affected by the flow of the fluids. The corrosion mechanism in the flowing conditions can be investigated in forced convection loop apparatus [2]. Molten salt LiF–NaF–KF (Flinak) has similar characteristics with Flibe. Flinak has potential to be used as simulator fluid for the flowing corrosion tests, and Flinak is also one of candidates of the coolant and tritium breeder of the blankets [3].

The corrosion characteristic of steels in a static Flibe has been investigated [4–6]. Reduced activation ferritic steel, JLF-1 (8.92Cr–2W) is candidate of structural material of the blanket. The data of corrosion in Flibe and Flinak is still limited.

In the present work, static corrosion tests were performed in Flibe and Flinak. Impurity such as oxide and H$_2$O in Flibe was removed by injection of HF and H$_2$ gas before the test. Flinak was not purified before the test, and Flinak contained H$_2$O. HF concentration in both fluids was measured by slurry pH titration method. The purpose of the present study is to investigate corrosion characteristics of JLF-1 steel in molten salts Flibe and Flinak.

2. Experimental conditions

2.1. Molten salts Flibe and Flinak

Flibe was the mixture of LiF and BeF$_2$ at the ratio of 34–66 mol.%, and purified by the injection of HF and H$_2$ gas. The metal impurity after the purification was shown with that after corrosion test in Table 1. HF concentration in Flibe was measured by slurry pH measurement method. Flibe was hardly dissolved in water. Then, slurry fluid was made of Flibe powder (1 g) and alcohol. After HF dissolved from the powder surface into alcohol, neutralize titration was performed using NaOH at the concentration of 0.1 mol/l. The accuracy for the HF measurement is 10 ppm. It was found that 180 ppm of HF was dissolved initially in Flibe.

The powder of LiF, NaF and KF was mixed at the ratio of 46.5–11.5–42 mol.%, and melted at 600 °C in air. Flinak of 200 g was prepared without the purification by gas injection as Flibe.

Table 1
Impurity of molten salts Flibe and Flinak.

	Impurity concentration (wppm)							
	Fe	Cr	Ni	Mo	Mn	W	Nb	HF
Flibe (initial)	70	5	16	<1	–	<1	–	180
After test A	260	130	37	1	88	12	–	170
After test B	300	810	70	1	120	8.7	–	190
Flinak (initial)	2	<0.1	140	0.6	<0.1	0.4	–	<10
After test C	1700	870	33	–	–	97	–	40
After test D	940	460	100	–	–	170	–	100
After test E	29	11	220	–	–	75	940	100

The melting point and heat of fusion was measured by differential scanning calorimeter (DSC2910 TA instrument). The melting point of 464.49 °C, and heat of fusion was 442.6 J/g. These data is close to those of Flibe, in which melting point is 458 °C and heat of fusion is 480 J/g [7]. HF concentration in Flinak was measured by above-mentioned method as the same as that in Flibe. Initial HF concentration in Flinak was less than 10 ppm. H_2O concentration was measured by Karl-Fischer titration. H_2O dissolved in Flinak was evaporated at 300 °C in the career gas of He, and moisture-He gas mixture was injected into Karl-Fischer reagent. It was found that the initial Flinak contained 16.1 wt.% of H_2O, and this is because Flinak absorbed H_2O in the process of mixing and melting in air.

2.2. Chemical potential of HF in molten salts

The chemical potential of HF for fluoridation in the fluids is expressed as:

$$\Delta G_f = \Delta G_{HF}^0 + RT \ln \frac{P_{HF}}{P}, \quad (1)$$

where ΔG_{HF}^0 is Gibbs free energy formation of HF, R is gas constant and T is temperature of the fluids with the unit of K. P_{HF} is partial pressure of HF in the fluids. It is known that Henry's law can apply to the correlation between partial pressure and the concentration in molten salts. Then, Eq. (1) can be derived as:

$$\Delta G_f = \Delta G_{HF}^0 + RT \ln \frac{C_{HF}}{C_s}, \quad (2)$$

where C_{HF} is the content of HF with the unit of ppm and C_s is the saturation concentration given by reference [8]. The estimated potential was shown with Gibbs free energy of formation of metal fluorides in Fig. 1. It was found that the fluoridation potential of Flibe with 180 ppm HF was larger than that of CrF_2 and FeF_2.

2.3. Corrosion test conditions

Corrosion test conditions are presented in Table 2. Test material is JLF-1, and the chemical composition is 8.92Cr–2.0W–0.2V–0.09C–Fe balanced (wt.%). The final annealing was normalizing at 1323 K for 1 hr and tempering at 1053 K for 1 hr. Specimen is rectangular plate type. The surface was mechanically polished to remove the oxide layer before the corrosion test. One specimen was placed in the crucible with 5 g molten salt, and then packed in capsule with 99.999% purity Ar gas. Fig. 2 shows schematic of test capsule. The material of crucible was one parameter to control the occurrence of electrical corrosion between the different materials. In tests C and D, two capsules were prepared to analyze without cleaning of specimen.

After the exposure, specimen was extracted from the crucible. Adhered molten salt on the specimen were melted and removed in the LiCl–KCl pool around 500 °C. The weight changes of specimens were measured by using electro reading balance with accuracy of 0.1 mg. The used molten salt was analyzed by ICP–MS. The process
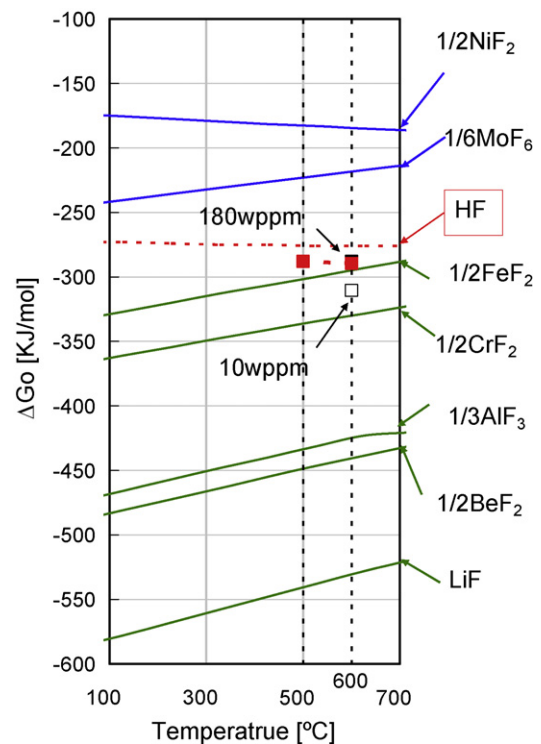

Fig. 1. Chemical potential of HF and Gibbs standard free energy of formation.

of capsule sealing and specimen extracting was done in globe box filled with Ar of 99.999% purity.

The specimen surface and cross section were analyzed by SEM/EDS. For the cross section analysis, electro etching was done
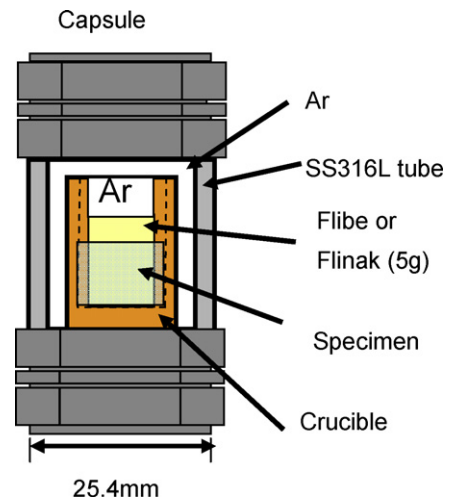

Fig. 2. Corrosion test capsule.

Table 2
Test conditions.

	Temperature	Materials		Number of cupsule
	(°C)	Specimen	Crucible	
Flibe				
Test A	500	JLF-1	JLF-1	1
Test B	600	JLF-1	JLF-1	1
Flinak				
Test C	600	JLF-1	JLF-1	2 (1) Cleaned after exposure (2) Not cleaned
Test D	600	JLF-1	Ni	2 (1) Cleaned after exposure (2) Not cleaned
Test E	600	JLF-1	Nb	1

at 30 V for 10 s in pool of 13%HClO$_4$–13%butoethanol–10%ethanol–64%acetic acid.

3. Results and discussion

Fig. 3(A) shows SEM image of the surface of solid Flinak. Fig. 3(B) shows the typical surface condition of specimens, and there was polish trace on the surface due to the mechanical polish. Fig. 3 (a)–(e) shows the specimen surface after the exposure. Fig. 4(a)–(e) shows the cross sectional SEM image and the EDS analysis results for the steel alloying elements. The metal impurities after the tests in the molten salts are shown in Table 1.

3.1. Corrosion in Flibe

The specimen had corrosion products, in which Cr was enriched and Fe and W were poor after the tests A and B. (Fig. 3(a) and (b)). These were not carbide because the carbide in JLF-1 was Cr-W carbide [9]. The change of Fe and Cr concentration in depth profile was small at 500 °C (Fig. 4(a)). On the contrary, the Cr concentration decreased at 600 °C, and Fe enriched (Fig. 4(b)). The depth was estimated around 5 μm.

It was found that the increase of Fe and Cr concentration in Flibe was large (Table 1). This is due to the dissolution of metal elements from the surfaces of specimen and crucible into Flibe in the corrosion process. Possible corrosion mechanism is:

$$Fe + 2HF \rightarrow FeF_2 + H_2, \tag{3}$$

$$Cr + 2HF \rightarrow CrF_2 + H_2. \tag{4}$$

CrF$_2$ is stabler than FeF$_2$ as shown in Fig. 1. Then, the corrosion of Eq. (4) might have occured first. After the depletion of Cr from the surface, the corrosion for Fe could be caused by fluoridation. The other possibility of the corrosion is due to the formation of Fe–Cr–fluoride.

In the test B, the number of carbide near the surface was less than normal part as shown in Fig. 4(b). This implied that C depleted from the surface due to the corrosion.
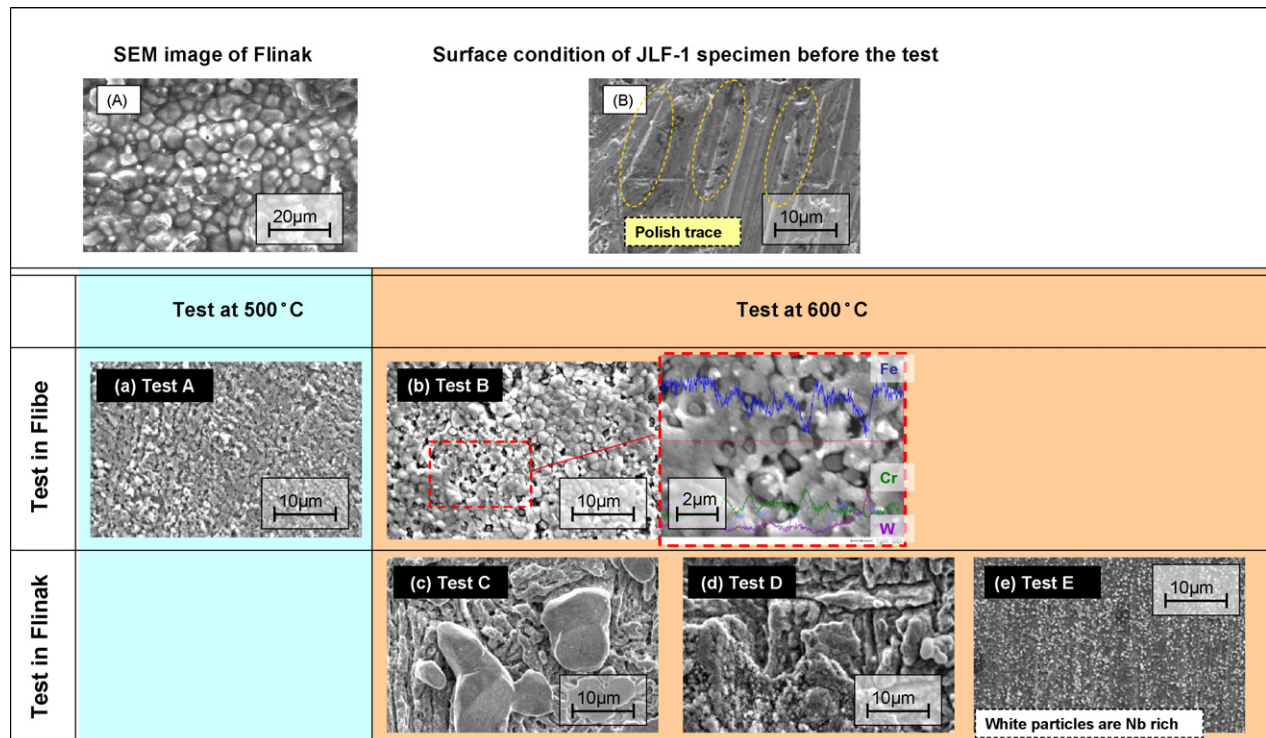

Fig. 3. SEM observation results for surface of (A) solid Flinak, and (B) JLF-1 before exposure, (a) JLF-1 after corrosion test A, (b) JLF-1 after corrosion test B, (c) JLF-1 after corrosion test C, (d) JLF-1 after corrosion test D, and (e) JLF-1 after corrosion test E.
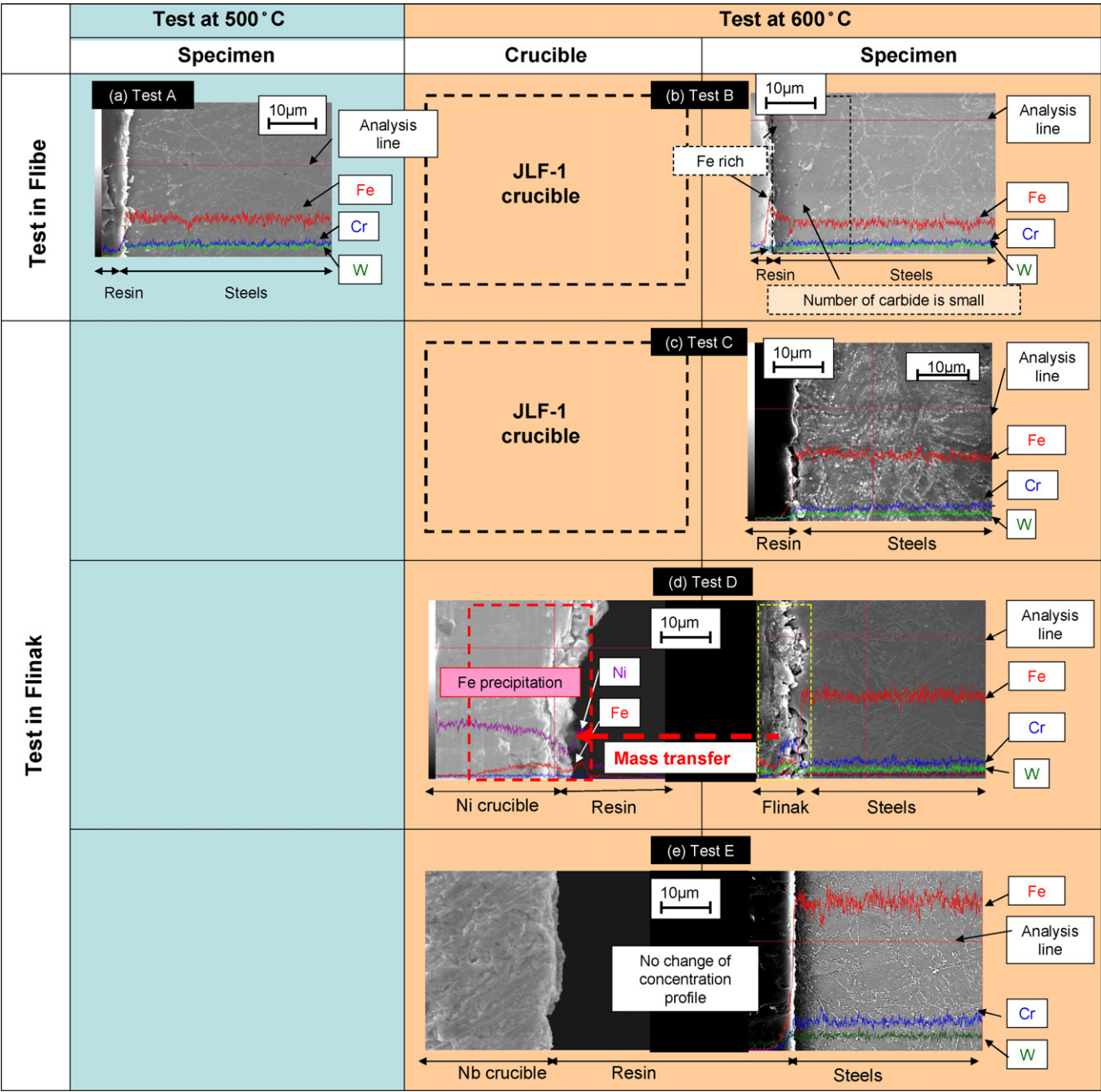
Fig. 4. SEM/EDS analysis results of surface cross section of JLF-1 after (a) test A, (b) test B, (c) test C, (d) test D and (e) test E.

The weight losses of the specimens were sufficiently small (Table 3). However, these values included the error by the adhered corrosion products. It was found that the concentration of HF in Flibe was not changed by the exposure (Table 2). HF must be used if the surface was fluorided by dissolved HF. In the test at 600 °C, HF of about 730 ppm had to be used according to Eqs. (3) and (4).

This data implied that HF could be generated during the exposure. If there was H_2O in Flibe and the concentration of HF decreased, small amount of HF can be generated by:

$$(Metal)F_2 + H_2O \rightarrow (Metal)O + 2HF. \tag{5}$$
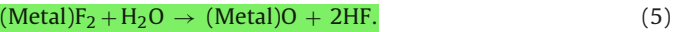
The reverse reaction of Eq. (5) was used to remove BeO and the other metal oxides by injection of HF gas in the purification process of Flibe. H_2O could be generated as

$$H_2 + (Metal)O \rightarrow H_2O. \tag{6}$$

3.2. Electrochemical corrosion in Flinak

HF concentration in Flinak increased in the corrosion test (Table 1). The corrosion by HF might be caused and Cr was depleted from the specimens. Initial Flinak containing H_2O of 16.1 wt.% may

Table 3
Corrosion depth of JLF-1 in molten salts obtained from weight losses.

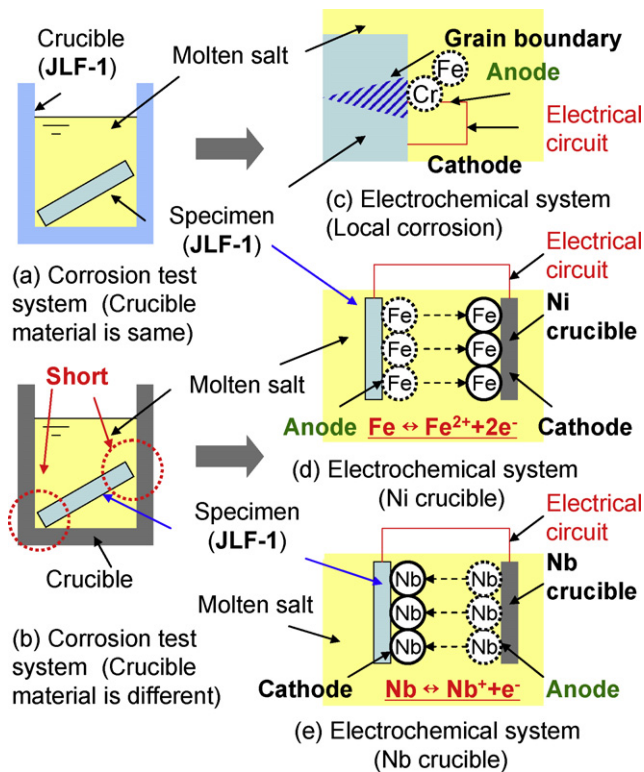|	Weight losses (g/m$_2$)	Corrosion depth (μm)
Test A	5.01	0.637
Test B	5.01	0.637
Test C	53.0	6.73
Test D	187	23.9
Test E	−0.661	−0.0840

Density of JLF-1: 7.80 g/cm^3

Fig. 5. Schematic presentation of electrochemical corrosion in molten salt Flinak.

generate HF during the corrosion test according to Eq. (5). This might result in large corrosion in Flinak.

The specimen surface had gap after the exposure in Flinak with JLF-1 or Ni crucibles (Fig. 3(c)). The gap width was approx. 2 μm and this was slightly larger than the lath width of 0.7 μm [10]. This indicated that the corrosion developed around the lath boundary. The depth profile of metal content showed small change of the element concentration, though the surface became rough by the exposure (Fig. 4(c) and (d)).

In the tests D and E, the crucible material was different from that of specimen. The electrochemical corrosion could be caused by different corrosion potential as shown in Fig. 5 [11]. The surface after the test D (Fig. 4(d)) was similar to that in test C. The cross sectional analysis was done in the specimen which was not cleaned. Fe and Cr were dissolved in the adhered Flinak (Fig. 4(d)). The dissolved Fe was alloyed with Ni on the crucible surface. When the electrochemical corrosion occurred in the fluids, corrosion rate became larger than that in the corrosion by impurity (Table 3).

In the test E, the particle of Nb was observed on the surface (Fig. 3(e)), and this Nb was dissolved from the crucible and precipitated on the specimen surface. Nb was selectively corroded, and the other element was not dissolved (Fig. 4(e) and Table 1). Then, the weight loss of specimen was small even though the error by adherence of Nb on the specimen surface has to be considered.

The electrode potentials of alloy element in Flibe at 600 °C were −0.45 V for Cr^{2+}/Cr, −0.08 V for Fe^{2+}/Fe, 0.37 V for Ni^{2+}/Ni and 0.64 V for Nb^{4+}/Nb. If Nb formed oxyion NbO^+_2, the potential is −0.66 V [12].

In Flinak–JLF-1 system, the grain and lath boundary were selectively corroded because the chemical component was different and became the anode due to less Cr concentration in the electrochemical system. Based on the galvanic series, Fe in JLF-1 was selectively dissolved in Flinak-Ni system. Nb dissolution in Flinak-Nb system might be caused by the formation of oxyion. Then, Nb crucible worked as sacrificial anode, and the specimen was not corroded.

4. Conclusion

Corrosion characteristics of JLF-1 steel (8.92Cr–2W) in molten salts Flibe and Flinak were investigated by static corrosion tests. Major conclusions are follows:

(1) HF concentration was measured by slurry pH titration method before and after the exposure. It was found that the concentration did not change after the exposure. This indicated HF generation from H_2O.
(2) The corrosion of JLF-1 in Flibe was mainly caused by Cr dissolution possibly due to the fluoridation by HF. C was also dissolved, and this decreased the number of carbide on the surface.
(3) The corrosion of Flinak was caused by electrochemical corrosion. The grain and lath boundary were selectively corroded because the chemical component was different and became the anode in the electrochemical system.

References

[1] A. Sagara, et al., Innovative liquid breeder blanket design activities in Japan, Fusion Sci. Technol. 47 (2005) 524–529.
[2] M. Kondo, T. Nagasaka, A. Sagara, N. Noda, T. Muroga, Annual Report of National Institute for Fusion Science, 2006, p. 445.
[3] H. Yamanishi, A. Sagara, Annual Report of National Institute for Fusion Science, April 1999–March 2000, p. 177.
[4] T. Nagasaka, M. Kondo, H. Nishimura, T. Muroga, N. Noda, Fluoridation and oxidation behavior of JLF-1 and NIFS-HEAT-2 low activation structural materials, J. Nucl. Mater. (in press).
[5] H. Nishimura, T. Terai, M. Yamawaki, S. Tanaka, A. Sagara, O. Motojima, J. Nucl. Mater. 307 (2002) 1355–1359.
[6] M. Kondo, T. Nagasaka, A. Sagara, N. Noda, T. Muroga, Q. Xu, M. Nagura, A. Suzuki, T. Terai, Metallurgical study on corrosion of austenitic steels in molten salt LiF-BeF$_2$ (Flibe), J. Nucl. Mater. (in press).
[7] JSME Data Book: Heat Transfer, 4th edition, Nihon Kikai Gakkai, Maruzen cooperation, (1986) (in Japanese).
[8] P.E. Field, J.H. Shaffer, The solubilities of hydrogen fluoride and deutirum fluoride in molten fluorides, J. Phys. Chem. 71 (1967) 3218–3222.
[9] X. Qi, M. Kondo, T. Nagasaka, T. Muroga, M. Nagura, Corrosion characteristics of low activation ferritic steel, JLF-1, in liquid lithium in static and thermal convection conditions, Fusion Eng. Des. 83 (2008) 1477–1482.
[10] N. Inoue, T. Muroga, A. Nishimura, O. Motojima, Correlation between microstructure and hardness of a low activation ferritic steel (JLF-1) weld joint, J. Nucl. Mater. 258–263 (1998) 1248–1252.
[11] K.A. Romberger, J. Braunstein, R.E. Thoma, New electrochemical measurements of the liquids in the LiF-BeF2 system. Congruency of Li$_2$BeF$_4$, J. Phys. Chem. 76 (1972) 1154–1159.
[12] C.F. BAES Jr., The chemicstry and thermodynamics of molten salt reactors fuels, J. Nucl. Mater. 51 (1974) 149–162.